

Inverse Lithography Technology (ILT)

Keep the balance between SRAF and MRC at 45 and 32 -nm

Linyong Pang, Yong Liu, Thuc Dam, Kresimir Mihic, Thomas Cecil, Dan Abrams
Luminescent Technologies, Inc.
2471 East Bayshore Road, Suite 600, CA 94301, USA
Phone: +1-650-433-1025 FAX: +1-650-960-3954 e-mail: leo@luminescent.com

ABSTRACT

In this paper, we present the Luminescent's ILT approach that can rapidly solve for the optimal photomask design. We will discuss the latest development of ILT at Luminescent in the areas of sub-resolution assist feature (SRAF) generation and optimization to improve process window, and mask rule compliance (MRC). Results collected internally and from customers demonstrate that ILT is not only an R&D tool, but also a tool quickly maturing for production qualification at advanced technology nodes. By enforcing the proper constraints while optimizing the masks, ILT can improve process windows while maintaining mask costs at a reasonable level.

Keywords: Lithography, Inverse Lithography Technology (ILT), Optical Proximity Correction (OPC), Resolution Enhancement Technology (RET), Sub-Resolution Assist Feature (SRAF), Mask Rule Compliance (MRC), photomask

1. INTRODUCTION

Increasingly, for semiconductor manufacturers moving to advanced nodes – 90nm, 65, 45, and below – the greatest challenge is lithography. This is because lithography is fundamentally constrained by basic principles of optical physics. At 65 nm and below, a line is less than a third of the effective wavelength of 193nm; optical diffraction and interference are becoming fundamental obstacles, not just second order effects.

It has long been known that the best lithography that is theoretically possible can be achieved by considering the design of photomasks as an inverse problem -- and then solving the inverse problem to find the optimal photomask for a given process, using a rigorous mathematical approach. Inverse Lithography Technology (ILT) has been explored for many years[1-8]. Although these early approaches to ILT often resulted in superb lithography, they were generally impractical in a production environment. Run-times were many orders of magnitude too slow, and the resulting masks were often too complex to manufacture.

By ILT we mean the following: given the known forward transformation of a lithography process, ILT mathematically determines the optimized mask which produces the desired wafer target with the best pattern fidelity and/or largest process window. The forward transformation is modeled accurately, which may take into account all of the elements of the transformation from mask to wafer: for example, the electromagnetics of the 3D mask, the optics of illumination and the lens, the behavior of the photoresist, the dose, focus conditions, aberrations, etc. However, the strict inverse problem is ill-posed; because the forward operator is many-to-one (that is, many different masks will yield identical on-wafer results), and the function has no well-defined inverse. Moreover, for typical target patterns (e.g., a drawn layout with Manhattan geometry and sharp corners), there does not exist any mask function which will produce the exact drawn wafer target. These issues are addressed by recasting the inverse problem as an optimization problem.

2. ILT AND ITS TECHNICAL ASPECTS

We define a merit function, also called a cost function, energy function, or Hamiltonian (by analogy to quantum mechanics). This function is indicative of the quality of the solution, or the "goodness" of the mask. In a simple case, the Hamiltonian could be the absolute value of the difference between the wafer image and the target pattern, integrated over the area of the mask. In practice, a number of additional elements may be included in the Hamiltonian. For example, the wafer pattern at various conditions throughout the process window (i.e., over or under exposed and/or plus/minus focus), the normalized image log slope (NILS) of the image, the robustness against mask error enhancement factor (MEEF), or other factors as deemed appropriate. The actual functional form may be different from the form as described above as

well. Elements that are not directly related to lithography may be included; for example, simple masks may be preferred over complex masks, and terms to this effect may be included in the Hamiltonian as well. What is essential is that the Hamiltonian is a functional of the mask function, and that minimizing said Hamiltonian allows us to find the optimal mask, according to the criteria we have chosen.

Our approach to ILT is based on a branch of mathematics invented by Stan Osher at UCLA. Commonly known as level-set methods[9], these techniques have been applied to the solution of inverse problems in a wide range of engineering disciplines such as image processing and fluid dynamics. The mask and wafer contours are represented by level-sets in such methods (Figure 1). The above formulation of the problem has a variety of advantageous properties. For example, the level-set representation allows for contours to merge, break, appear, or disappear, in a consistent, mathematical representation. Various functions (for example, the wafer image) can be determined as closed form expressions. The mask function itself is an element of a Hilbert-space which is much larger than the two-dimensional space of the photomask, which allows for “more global” solutions to be found.

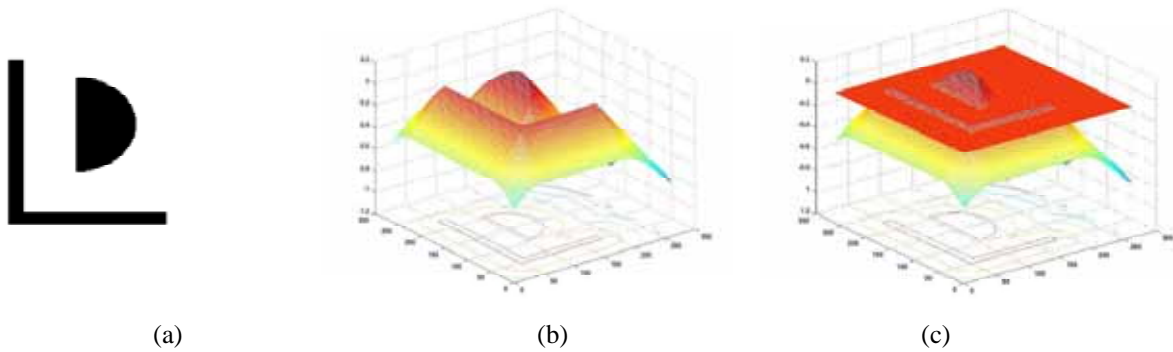


Figure 1. The level-set representation of mask problem, where (a) is a mask pattern, (b) is a distance function (the value of function represents the distance from the location to the mask edge), and (c) is the level set (The intersection of “0” level set with distance function represents the mask contour).

Another important aspect of the minimization problem comes in the form of constraints. A variety of constraints are imposed by the realities of mask manufacturing; for example, two disjoint chrome regions must be separated by a minimum distance, and a chrome line must have a minimum width. We address these constraints by defining a sub-space of the full Hilbert space of mask functions, and restricting our solution to this sub-space.

A key distinctive feature of ILT is the absence of pattern-dependent heuristics, and the ability to broadly explore wide areas of solution space. ILT algorithms frequently lead to mask patterns which are unanticipated by a knowledgeable practitioner. As will be shown in the next example of the problem of placement of sub-resolution assist features (SRAFs), there are mask features that do not print on the wafer which are detached from the edges of the main mask patterns, and yet manipulate the light reaching the wafer so as to accentuate the wafer image. In the past, these were placed empirically, with great care, and frozen in place during the computation of the rest of the mask. In contrast, ILT can determine optimal SRAFs simultaneously with the rest of the mask. The absence of segmentation scripts is a significant advantage because it usually requires significant engineering resources to write such scripts for different patterns on different design layers.

Figure 2 shows an example to demonstrate the power and flexibility of ILT [10]. The goal is to print a regular contact array with 110nm CD, 440nm pitch. The numerical aperture of the stepper is 0.78, the illumination source is a disk with a sigma of 0.3. In Figure 2 we show a continuous tone mask, an attenuated phase-shifting mask without mask constraints, and an attenuated phase-shifting mask with Manhattan constraints, all designed with ILT, to print the above described contact hole array. The process window of images produced by the Manhattan attenuated phase-shifting mask gives a DOF of 574 nm at 7% exposure latitude. The aerial image contrast is 0.85, well above 0.35, which is the rule-of-thumb minimum aerial image contrast required to print on wafer. It is quite remarkable that the combination of a single small central region, with four distinct surrounding lobes, should optimally print the contact pattern. Such remarkable patterns illustrate the power of ILT, which finds solutions that are often unexpected. Notice also the assist features found further away the contact, around the perimeter of the image.

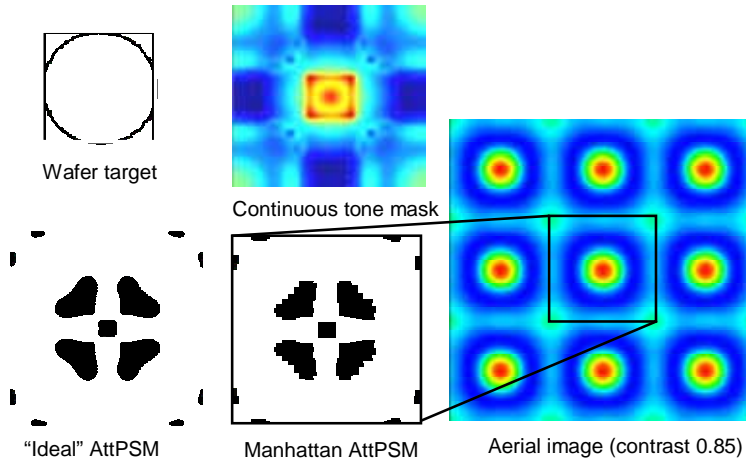


Figure 2. ILT contact array example: contact target of 110nm CD, 440nm pitch. Three types of masks were generated from ILT: continuous tone mask, “ideal” attenuated phase-shifting mask, attenuated phase-shifting mask with Manhattan constraints, and the aerial image simulated using Manhattan AttPSM.

By finding the more global optimized mask patterns, ILT brings an additional benefit of improved wafer pattern fidelity and process window. It also opens the possibility of using existing lithography equipments (e.g., scanner) into smaller geometries; in other words, extending the life of existing lithography equipments.

Using modern numerical methods and the latest processors, it is now possible to quickly solve the resulting minimization problem. Our implementation divides a large photomask into small regions called “work units”. These are distributed to a cluster of compute nodes, which can then process many work units in parallel. The solutions are then stitched together to form a complete mask. A large number of real full-chip designs have been processed this way through our system. The results can thereby be obtained quite quickly. In one recent example, a large 4 cm² die (wafer scale) was processed overnight.

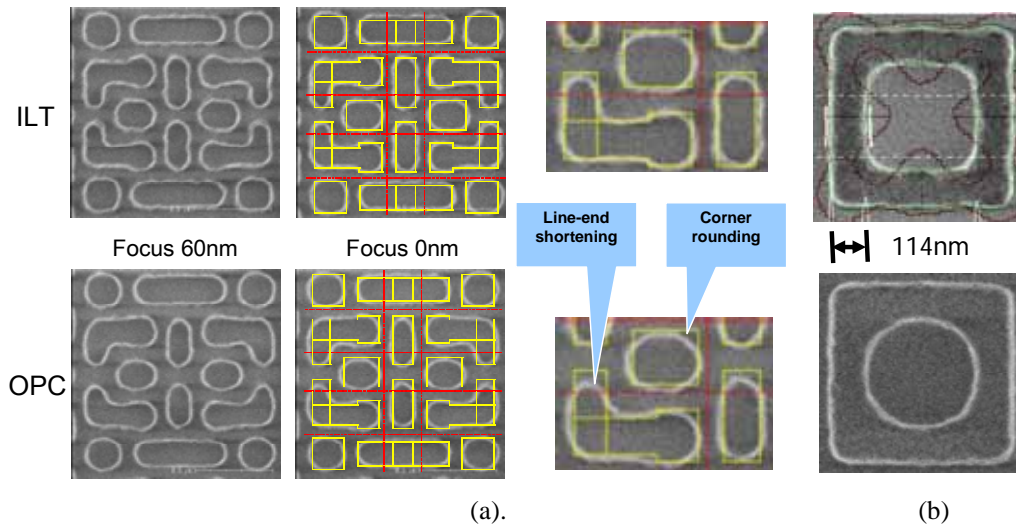


Figure 3. ILT and OPC wafer images. (a). Through focus wafer patterns of metal 1 layer, where outline is the design target. The insets at right are a magnification of a selected portion of the 0nm focus condition. (b). a square “donut” shape (CD 114nm on wafer).

Figure 3 shows wafer prints of clips of ILT optimized full-chip masks one world leading foundry. The result on the left (Figure 3(a)) is from a 65nm metal 1 layer[11]. In this case, both ILT and OPC used optical model. Two images for both ILT and OPC were captured at best focus, and at plus 60nm defocus. It shows wafer image using ILT mask has better pattern fidelity through process window. From the zoomed-in pictures (insets at right), it is clear that ILT produces less

line-end shortening and corner rounding issues. The result on the right (Figure 3(b)) is from another test mask and test wafer[12]. The design target is a square “donut” shape with very small dimension (CD 114nm on wafer). From the inner shape of the “donut” it is clear ILT can resolve smaller features better than OPC in this case.

3. CLARIFICATION OF SOME COMMON MYTHS ABOUT ILT

There are also some common myths associated with ILT. One of these is that ILT always results in a unique global optimum. Although this may be true for some algorithms, many inverse lithography approaches are based on local search heuristics which find a good -- but not necessarily global -- optimum. Moreover, because the inverse problem is mathematically ill-posed, there are many situations in which the global optimum is not unique. It is then up to the algorithm (or algorithm designer) to determine which of many equally good solutions is desired.

Another ILT myth is that such methods must be image or pixel based. The algorithm developed at Luminescent and discussed below is pixel based, but not every approach to inverse lithography necessarily is.

One of the common myths is that ILT cannot change the basic resolution physics and therefore cannot improve the fundamental resolution. This is not correct. First, the resolution is determined by how many orders of diffraction that a pattern can receive through the stepper optical system. If only zero order diffraction is received at the wafer image plane, then one would only see a constant background, in other words, the pattern cannot be resolved. That is the fundamental limitation of resolution. There are two common practices to increase the number of diffractions at the wafer image plane: using off axis illumination (OAI) or using phase shift mask. The applications of these approaches were extensively explored in the last two decades because the computation required is manageable by human beings. However, there is a third approach which is less popular and has only been explored recently – using the interaction of diffraction on mask patterns. SRAF can be considered as the first try in this approach for simple isolated line patterns. To make this approach applicable to complicated random patterns on the real chip designs, a fast inverse lithography computation engine is required. Second, for each generation, the resolution is actually not limited by the dense line/space patterns; in reality, it is the line-end and other features that limit the lithography capability. For example, in the SRAM core, resolving the line/space is not an issue; the issue is how to break line/space into small segments. ILT can help in such cases, because it requires a sophisticated consideration of shapes in surrounding area to properly manage the constructive and destructive interferences of higher order diffractions. Third, the K1 factor that a foundry feels comfortable to use is usually larger than 0.38, which is high; such K1 factor is calculated from dense line/space patterns. The reason such high K1 factor is required is that the other geometries, such as line/end, have smaller K1 factor, and foundries have to consider all types of geometries to be safe. ILT is the best way to utilize higher diffraction orders for random geometries. With ILT, the lithography capability can be extended to its ultimate limits.

Finally, there is a common perception that inverse lithography algorithms must represent a solution in closed form, or are in some sense direct solutions to the problem. In point of fact, however, most ILT methods that have been developed are iterative at some level, and it is quite true in general that engineering inverse problems are often solved with iterative methods. This should not be surprising, because many (if not most) modern mathematical solvers involve iterations, and, done properly, such methods can be very efficient.

4. LATEST DEVELOPMENT IN ILT

4.1 SRAF GENERATION

SRAF is commonly used in RET. There are three major problems in the current SRAF generation: 1) SRAF placements are primarily rule-based, and the rules are created using simple regular patterns, such as lines/spaces, or contacts with different pitches. Such rule might not be applicable or accurate for complicated geometries in a real design; 2) SRAF generation and OPC are two separate processes – first the SRAFs are generated and then OPC is run. This can be time consuming. 3) OPC only applies to main pattern. SRAFs usually are not optimized during OPC. 4) Side lobes that could print are difficult to detect and fix.

In ILT, SRAFs are automatically generated during the inversion calculation, and they are optimized simultaneously with the main features. Therefore, the SRAF generation becomes a straight forward, single-step process. Since every pixel is considered in the computation in the pixel-based ILT implementation, the issue of side-lobe-printing which has been a problem for edge-based OPC due to its edge-sampling-based approach can be effectively eliminated.

To illustrate auto SRAF features described above, three examples will be shown in the following (Figure 4, 5, and 6): one line/space sequence, one real contact layer pattern, and one trench pattern. In the first example, a simple line/space pattern with varying pitch is used as the target. The line CD in this sequence is kept as 70 nm, but the pitch is varied from 210nm to 800nm; therefore, this pattern covers dense, semi-dense, and nearly isolated conditions.

In the current OPC approach, some simple rules are usually created to facilitate addition of SRAFs for line/space patterns; for instance, if the space between two adjacent line/space is smaller than a certain size, no SRAF; if the space is larger than certain size, add one SRAF with a certain size at a certain distance; if the space is larger than another distance, add two SRAFs, etc. In general, the number of SRAFs, whether to add them, the SRAF location and dimension are all pre-defined based on simple rules.

Figure 4(a) shows a sequence of line/space target pattern and post-correction patterns from ILT, including SRAFs, to give the optimized wafer printing performance. Comparing with OPC approach, one can notice some distinguishing properties of SRAFs generated by ILT: the number of SRAFs depends on the pitch; and the location and size of SRAFs change when pitch changes even for pitches where the number of SRAFs stays constant. Figure 4(b) shows the depth of focus (DOF) at 6% exposure latitude (EL) for this line/space pattern sequence. The DOF curve for line/space correction without SRAF shows the DOF drops as pitches increases; With insertion of SRAFs, DOF approaches a constant after the space is large enough for first SRAF insertion.

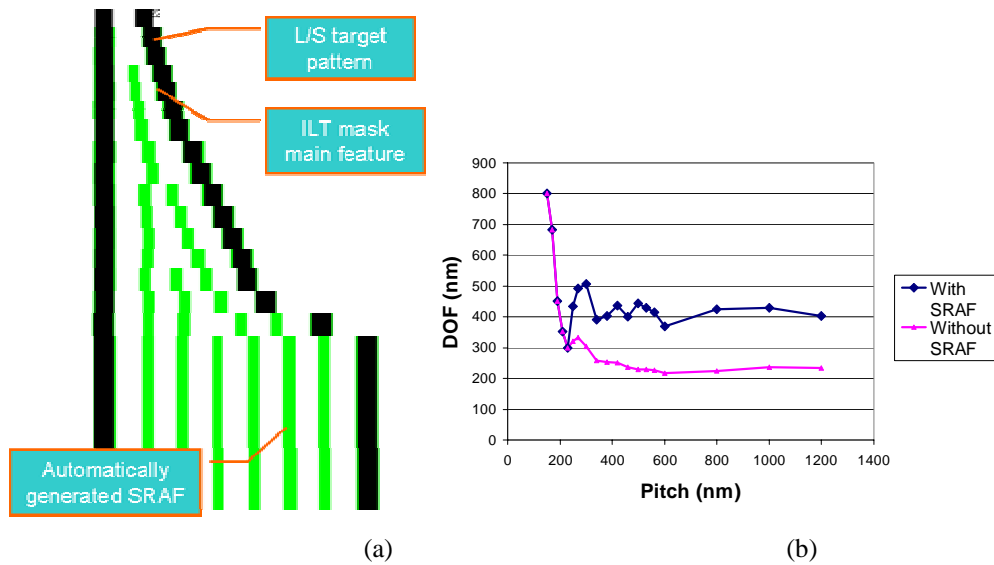


Figure.4. Simultaneous mask creation and SRAF placement using ILT for a sequence of pitches of clear field line/space patterns. (a) shows the line/space target (black) and ILT generated mask patterns (green/gray), including main features and SRAFs. (b) shows the DOF for through pitch patterns optimized with ILT with and without SRAF

The example above contains only simple line-space, the next example (Figure 5) shows a real layout pattern, a 45nm random logic contact layer. Since the arrangement of the contact is random, the conventional simple rule-based SRAF placement in OPC leads to many conflicts, such as overlapped SRAFs etc., that are not covered by the rules. Resolution of those conflicts is very difficult under the framework of current OPC approaches. ILT solves this problem by simultaneously optimizing both SRAF and main feature. Some SRAFs generated by this approach is inconceivable under current OPC scheme. Since both main features and SRAFs are simultaneously optimized (including their shape, size, and location) during the inversion process, the SRAF generation process is very natural for ILT. The area enclosed by the red circle in Figure 5 is an example where rule-based SRAF has difficulties. Although not shown in the figure, no side lobes are present in operating ranges, despite the presence of quite large SRAFs.

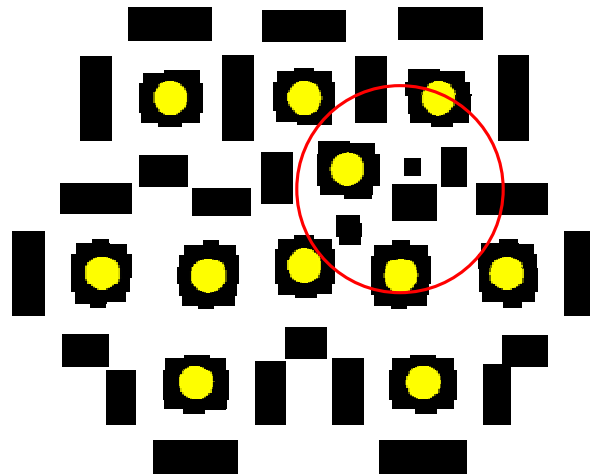


Figure 5. ILT automatically generated SRAF for a 45nm random logic contact layer, where the solid yellow represents the simulated contact shape on wafer, and the solid black represents the mask pattern calculated by ILT including both main features and SRAFs.

The next example (shown in Figure 6) is a 45nm non-contact layer example. This is a trench layer with 6 lines with different CD. Due to the subtle differences on the CD and the different locations in the arrangement, the line-end corrections on the main features are all slightly different in term of both shape and symmetry. In addition, the size and location of the SRAFs are also slightly different. Another interesting observation is on the SRAFs between the line-ends – both the line width and length of these SRAFs are also adaptive depending on the different CD of both trench patterns on the top and the bottom.

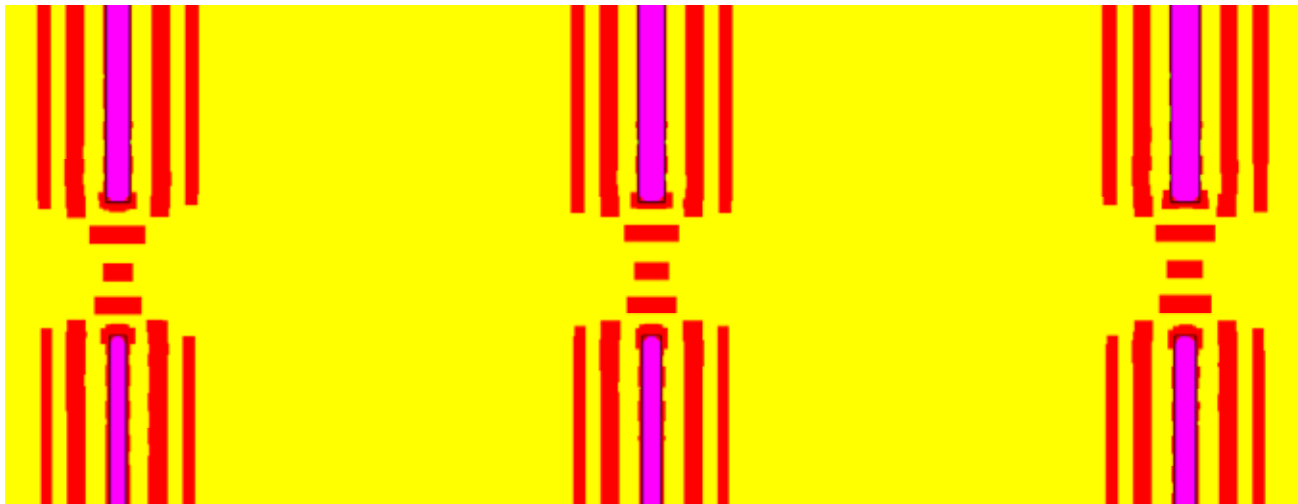


Figure 6. ILT automatically generated SRAFs for a 45nm trench layer, where the filled solid purple color represents the simulated trench shape on wafer, the un-filled black polygon represents the GDS drawn target, and the solid red color represents the mask pattern calculated by ILT including both main features and SRAFs.

4.2 PROCESS WINDOW ILT

Most OPC software optimizes masks at the nominal process condition to seek the best pattern fidelity (the smallest edge placement error (EPE)) on a single image plane (best focus and nominal exposure). This worked well at 130nm and 90nm technology nodes when the process window, especially the depth of focus (DOF) was relatively large. This is not adequate, however, at the 45nm technology node and beyond. A mask optimized for nominal condition may cause

bridging or pinching at slightly different exposure or focus. Such problems (called “hotspots”) are conventionally caught by verification systems after OPC, and fixed manually at the OPC script level. Often, this process of detection and re-scripting has to be repeated several times.

The process window “hot-spot” can be avoided in many cases, because there exist solutions that give the same EPE at nominal but improved defocus behavior. In the latest development of ILT, the process window margin is improved in two ways[13]: 1) Using multiple process conditions besides the nominal condition in the inversion calculation; 2) Adding terms directly related to DOF into the cost function.

In the following example shown in Figure 7, one was able to optimize both illumination source and mask to improve process window with ILT. The DOF for this challenging contact layer in a 45nm memory core improved from less than 300nm to more than 400nm, and at the same time allowing the use of a less expensive stepper (smaller NA).

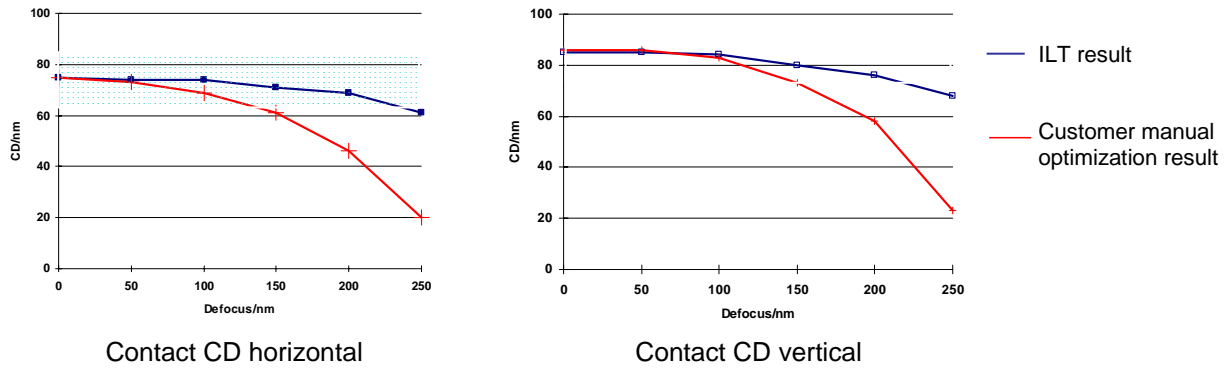


Figure 7. Comparison of simulated wafer CD values through focus in both horizontal and vertical directions between an ILT mask and a customer-manually-optimized mask for a tilted 45nm contact hole array.

4.3 MANHATTAN MASKS AND MRC IN INVERSION

In previous ILT implementations, the mask constraints were not considered, resulting in masks with curved geometry and many small fragments. Such masks are challenging for mask writing, inspection, metrology, and repair. With Luminiscent’s new ILT approach, the mask constraints are built into the inversion solver[14]. Users can specify mask rules, such as minimum CD, minimum space, minimum area, and minimum fragment length on the Manhattan shaped mask.

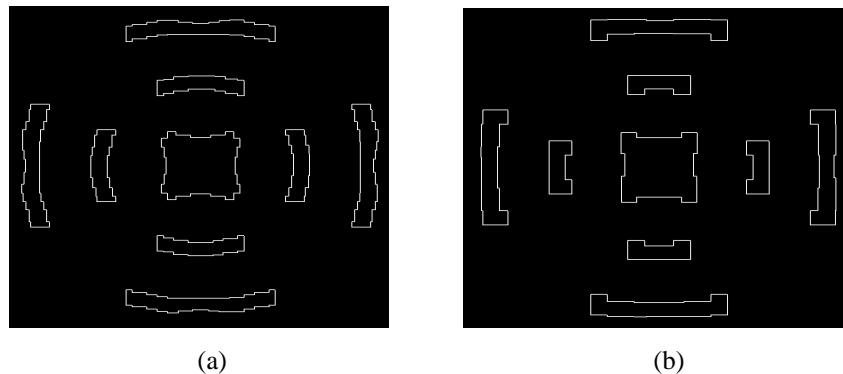


Figure 8. ILT mask patterns for isolated contact with different user specified mask rules: (a) min. fragment length 20nm, min. line/space 25nm; (b) min. fragment length 50nm, min. line/space 50nm .

As shown in Figure 8, the user can specify different mask rules, in this case, the minimum fragment length 20nm in 8a, 50nm in 8b, and minimum line and space both 25nm at wafer scale. The ILT program will generate different patterns optimized based on the user specified settings.

Mask rules can also be enforced with ILT. During the inversion calculation, mask rules, especially minimum line, space, and area are checked. The resulting mask is constrained by the specified mask rules. For example, as shown in Figure 9, without mask rule being enforced, the inversion may link two mask features together, creating a piece violating the minimum linewidth rule (Figure 9(a)). However, when mask rules are enforced during inversion, the algorithm won't allow such violation to happen, it generates instead a different shape of mask pattern that satisfies the minimum width and spacing mask rules (Figure 9(b)). Besides enforcing mask rules, features for fast mask data fracturing and writing time using VSB e-beam writers are also implemented. Again shown in Figure 9 (b), observing the Manhattanized mask, represented by black line, the vertices are aligned either in horizontal direction or vertical direction so that the number of e-beam figures are reduced.

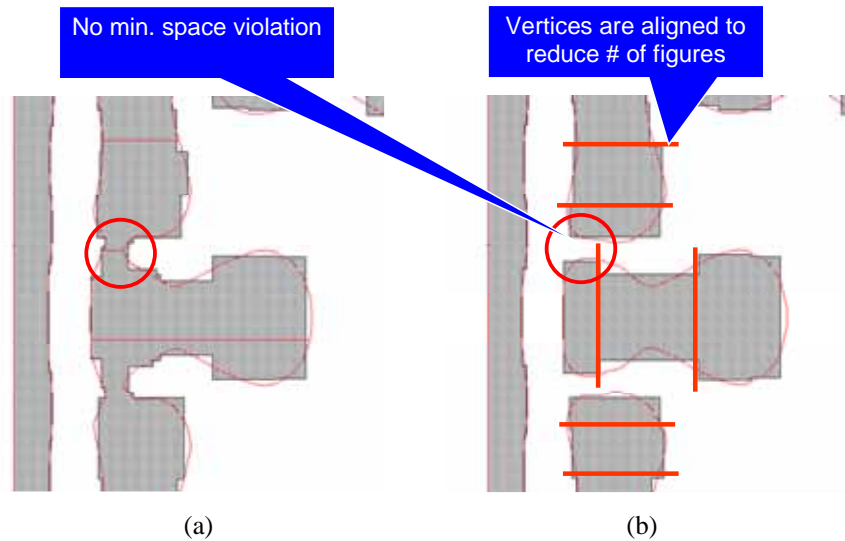


Figure 9. An example showing (a) mask pattern calculated with minimum linewidth rule not enforced, and (b) mask pattern calculated with minimum linewidth and space rules enforced. The red contour represents the “ideal” ILT mask pattern without Manhattan constrains, and the black line represents the ILT mask patterns with Manhattan constrains.

4.4 THE BALANCE BETWEEN SRAF AND MASK COST

In general SRAFs are smaller than the minimum CD in the design for each generation. Adding SRAF will increase number of figures on the mask, and the area of most of such additional figures are small, therefore, increasing the mask write time and the difficulty for mask inspection. Because of this, keeping the balance between SRAF and mask cost is important for applying ILT with SRAFs into production.

In our pixel-based ILT implementation, a rectangular strength is introduced to control how SRAFs are close to a rectangular shape. By varying the value of this single rectangular strength parameter, SRAFs can change from their ideal shapes to single shot rectangular shapes. For instance, the SRAFs for an isolated contact under annular illumination can change from circular shapes to four single shot rectangles in the north, south, east and west direction. Since this variable has continuous values from 0 to 1, user can turn this knob, and find the best tradeoff between mask complexity and wafer process window improvement.

The following example in Figure 10 demonstrates ILT mask patterns with SRAFs generated with different rectangular strengths. Two small clips from a large piece of contact layer are shown in the figure - one is single contact in an almost isolated environment, and the other includes two dense arrays of contact. Mask patterns with SRAF at three different

rectangular strengths are illustrated here. One can see the mask pattern complexity, especially in term of the number of figures for VSB mask writer, is different between these three configurations.

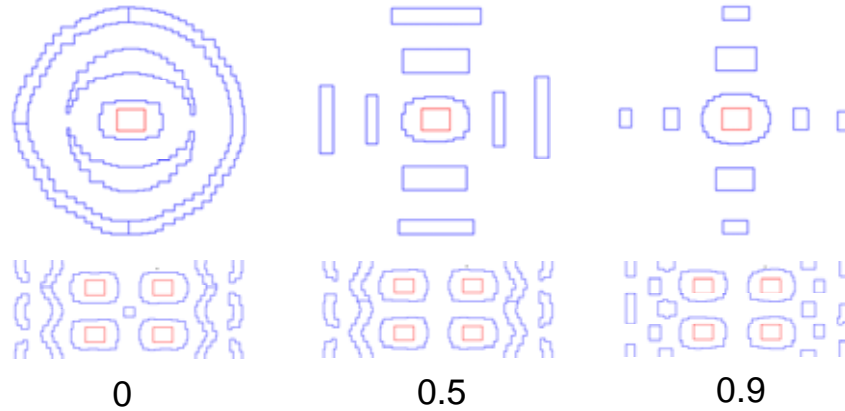


Figure 11 shows ILT mask patterns with SRAF generated at different rectangular strengths for an isolated contact and a nested array of contact in a large contact clip.

The SRAFs complexity not only affects the mask cost, but also affects the OPC quality in term of Edge-Placement-Error (EPE) and process window, such as Depth Of Focus (DOF). In general, reducing the SRAFs complexity will lose EPE and DOF in some level. Finding the best tradeoff between these two is critical to apply ILT with SRAFs into production. The rectangular strength parameter, in addition to mask rules, gives user the full control to find the optima between mask cost and process window improvement using SRAFs. Figure 12 shows the EPE and common DOF at different rectangular strengths for the contact clips of Figure 11. One can see a good tradeoff does exist at rectangular strength around 0.4, which the EPE and DOF do not lose much comparing with rectangular strength 0, while the mask is already much simplified.

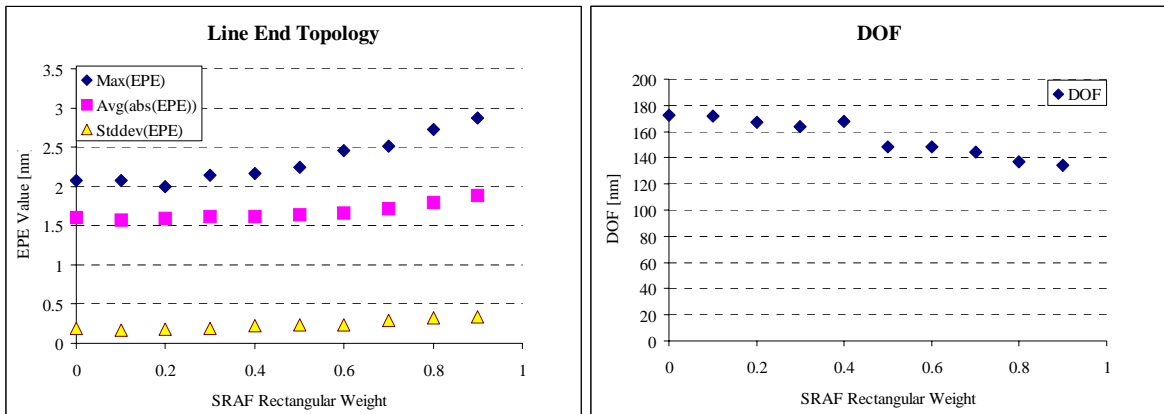


Figure 12. EPE and common DOF for ILT mask patterns with SRAFs in Figure 11 at different rectangular strength.

5. SUMMARY AND CONCLUSIONS

Inverse lithography technology has enjoyed significant advances. In particular, the implementation by Luminescent technology utilizing new advances in numerical computation such as level sets possesses many desirable features. It is able to design unique mask patterns that are inconceivable using traditional OPC. It has been shown to have enhanced pattern fidelity on wafer over existing technologies. It can be and had been formulated to optimize main features and SRAFs at the same time. In addition, enforcement of mask rules for the ease of manufacturability is effectively incorporated into the optimization algorithm, so that masks with Manhattan edges that satisfy mask rule constraints are generated. User is able to control the complexity of SRAF to best tradeoff the process window improvement and mask cost. The most delightful observation is that masks with those constraints continue to exhibit the unique features of ILT.

6. ACKNOWLEDGEMENT

The authors would like to thank the whole Luminescent team for creating the ILT implementation that made this work possible. The authors would especially like to thank Grace Dai for her help in preparing ILT mask patterns for this presentation, and thank Yoshio Tanaka, and Bob Gleason for reviewing the manuscript

REFERENCES

- ¹ B.E.A. Saleh and S.I. Sayegh, Reductions of errors of microphotographic reproductions by optical corrections of original masks, *Optical Eng.* Vol. 20 pp 781-784 (1981)
- ² K.M. Nashold and B.E.A. Saleh, Image construction through diffraction-limited high-contrast imaging systems: an iterative approach, *J. Opt. Soc. Am.A*, vol. 2 p. 635 (1985)
- ³ Y. Liu and A. Zachor, Optimal binary image design for optical lithography, *Proc. SPIE* Vol. 1264 pp 410-412 (1990)
- ⁴ Y. Liu and A. Zachor, Binary and phase-shifting image design for optical lithography, *Proc. SPIE* Vol. 1463 pp 382-399 (1991)
- ⁵ Y-T Wang, Y.C. Pati, H. Watanabe and T. Kailath, Automated design of halftoned double-exposure phase-shifting masks, *Proc. SPIE* Vol. 2440 pp 290-301 (1995)
- ⁶ S-H Jang et. al, Manufacturability evaluation of model-based OPC masks, *Proc. SPIE* vol. 4889 p 520 (2002)
- ⁷ A. Rosenbluth et. al, Optimum mask and source patterns to print a given shape, *JM3* vol. 1 pp 13-30 (2002)
- ⁸ T. Fuhner and A. Erdmann, Improved mask and source representations for automatic optimization of lithographic process conditions using a genetic algorithm, *Proc. SPIE* Vol. 5754 pp 415-426 (2005)
- ⁹ S. Osher and J. A. Sethian, Fronts Propagating with Curvature-Dependent Speed: Algorithms Based o Hamilton-Jacobi Formulations, *Journal of Computational Physics* 79, pp 12-49 (1988)
- ¹⁰ D. Abrams and L. Pang, Fast Inverse Lithography Technology, 31st Internal Symposium of Microlithography, *Proc. of SPIE* Vol. 6154, San Jose, California, USA, Feb. 2006
- ¹¹ C. Y. Hung, et al, Pushing the Lithography Limit: Applying Inverse Lithography Technology (ILT) at 65nm generation [6154-58], 31st Internal Symposium of Microlithography, *Proc. of SPIE* Vol. 6154, San Jose, California, USA, Feb. 2006
- ¹² B. Lin, et al, Inverse Lithography Technology at Chip Scale, 31st Internal Symposium of Microlithography, *Proc. of SPIE* Vol. 6154, San Jose, California, USA, Feb. 2006
- ¹³ Y. Liu, et al, Inverse Lithography Technology Principles in Practice: Unintuitive Patterns, 25th Annual BACUS Symposium on Photomask Technology, *Proc. of SPIE* Vol. 5992, Monterey, California, USA, Oct. 2005
- ¹⁴ L. Pang, et al, Inverse Lithography Technology (ILT), What is the Impact to Photomask Industry? Photomask Japan, Yokohama, Japan, April, 2006